






Article

Morphological and Phylogenetic Study of Protococcidians Sheds Light on the Evolution of Epicellular Parasitism in Sporozoa (Apicomplexa), with the Description of *Eleutheroschizon planoratum* sp. nov

Gita G. Paskerova ^{1,*}, Tatiana S. Mirolubova ², Andrea Valigurová ³, Vladimir V. Aleoshin ^{4,5}
and Timur G. Simdyanov ⁶

- ¹ Department of Invertebrate Zoology, Faculty of Biology, Saint-Petersburg University, Universitetskaya emb. 7/9, 199034 St. Petersburg, Russia
- ² Laboratory for Fauna and Systematics of Parasites, Center for Parasitology, Severtsov Institute of Ecology and Evolution, Russian Academy of Sciences, 119071 Moscow, Russia; provorosenok@gmail.com
- ³ Department of Botany and Zoology, Faculty of Science, Masaryk University, 61137 Brno, Czech Republic; andreav@sci.muni.cz
- ⁴ Belozersky Institute for Physico-Chemical Biology, Lomonosov Moscow State University, 119991 Moscow, Russia; aleshin@belozersky.msu.ru
- ⁵ Kharkevich Institute for Information Transmission Problems, Russian Academy of Sciences, 127051 Moscow, Russia
- ⁶ Department of Invertebrate Zoology, Faculty of Biology, Lomonosov Moscow State University, 119234 Moscow, Russia; tgsimd@gmail.com
- * Correspondence: gitapasker@yahoo.com or g.paskerova@spbu.ru



check for updates

Citation: Paskerova, G.G.; Mirolubova, T.S.; Valigurová, A.; Aleoshin, V.V.; Simdyanov, T.G. Morphological and Phylogenetic Study of Protococcidians Sheds Light on the Evolution of Epicellular Parasitism in Sporozoa (Apicomplexa), with the Description of *Eleutheroschizon planoratum* sp. nov. *Diversity* **2023**, *15*, 863. <https://doi.org/10.3390/d15070863>

Academic Editors: Michael Wink, Martina Schrallhammer and Alexey Potekhin

Received: 30 May 2023
Revised: 27 June 2023
Accepted: 13 July 2023
Published: 17 July 2023



Copyright: © 2023 by the authors. Licensee MDPI, Basel, Switzerland. This article is an open access article distributed under the terms and conditions of the Creative Commons Attribution (CC BY) license (<https://creativecommons.org/licenses/by/4.0/>).

Abstract: The order Protococcidiida is one of the most poorly studied basal groups of Sporozoa (Apicomplexa sensu stricto). To date, the phylogenetic unity of protococcidians and their relationship with other sporozoans are understudied. Only the protococcidian *Eleutheroschizon duboscqi* has molecular evidence of a sister position to “true” coccidians (*Eimeria*, *Sarcocystis*, *Toxoplasma*). *E. duboscqi* is characterized by epicellular development in the so-called parasitophorous sac of the host cell origin. The unusual localization of *Eleutheroschizon* is comparable to that of *Cryptosporidium*. We describe a new species of the genus, *E. planoratum* ex *Naineris quadricuspida* polychaete from the White Sea, using light and electron microscopy. The morphology of attachment apparatus, phylogenetic analyses of concatenated DNA sequences of the nuclear ribosomal operon (SSU rDNA, ITS1, 5.8S rDNA, ITS2, and LSU rDNA), and compensatory base changes in ITS2 secondary structures of both protococcidians confirm the new species. The resulting phylogenies also confirm that *Eleutheroschizon* is sister to eimeriid coccidians, while *Cryptosporidium* tends to be grouped with gregarines. We discuss a new type of endoparasitism among sporozoans—the closed epicellular parasitism that evolved convergently in *Eleutheroschizon* and *Cryptosporidium*. The diagnosis of the new species and the emended diagnoses of the species *E. duboscqi* and the genus *Eleutheroschizon* are presented.

Keywords: marine apicomplexans; host–parasite interactions; *Cryptosporidium*; Eleutheroschizonidae; Protococcidiida; polychaetes; intestinal parasites; coccidians

1. Introduction

One of the poorly studied basal groups of Sporozoa (Apicomplexa sensu stricto; see [1,2]) is the order Protococcidiida Kheisin, 1956. This group currently includes five families: Coelotrophidae Vivier, 1981; Eleutheroschizonidae Chatton and Villeneuve, 1936; Myriosporidae Grasse, 1953; Angeiocystidae Léger, 1911; and Grelliididae Levine, 1973. Protococcidians parasitize in invertebrates (mainly marine) and are characterized by the absence of merogony and the presence of extracellular gamogony and sporogony in their life cycle [3,4]. To date, the phylogenetic unity of protococcidians and their relationship to other

sporozoans have not been confirmed via molecular biological methods. An exception is *Eleutheroschizon duboscqi* Brasil, 1906, whose phylogenetic position as a sister branch to “true” coccidians (*Eimeria*, *Sarcocystis*, and *Toxoplasma*) was demonstrated using multiprotein phylogeny [1]. This was later supported by other multimarker phylogenies [5–7]. *E. duboscqi* is characterized by cell polarity and epicellular development on the host intestinal epithelium. Epicellular trophozoites develop into gamonts of two types, macrogamonts and microgamonts. Macrogamonts have one large nucleus, while microgamonts possess several small nuclei. As gamonts develop, they detach from the host cells and are released with successive gametogony (macrogamont transforms into a macrogamete, while microgamont gives rise to several microgametes) and sporogony into seawater. Oocysts contain fan-shaped clusters of sporozoites connected at one end to a residual body [4,8,9]. Currently, two species are known within the genus: the type species *E. duboscqi* from the polychaete *Scoloplos armiger* (Müller, 1776), and *E. murmanicum* Awerinzew, 1908 from the polychaete *Ophelia limacina* (Rathke, 1843).

In addition to previous light-microscopic studies on *E. duboscqi* [8,9], the endogenous (trophozoite and gamont) stages of this parasite were found in the intestines of *S. armiger* polychaetes from the White Sea littoral and studied using modern light, confocal and electron microscopy [10]. This study showed that *E. duboscqi* develops in the parasitophorous sac. The parasitophorous sac, previously described for cryptosporidians [11], is an epicellular structure (niche) formed by the host cell, enveloping the entire parasite. It consists of two continuous host plasma membranes on the outer and inner sides and a thin layer of host cell cytoplasm between them. The unmodified and modified parts of the host cell are separated by a dense band of microfilaments. The parasitophorous sac forms a caudal appendage (“tail”) over the posterior end of the parasite and has pores on its surface. Parasites have a morphologically pronounced attachment apparatus. It consists of outgrowths (lobes) arranged in one or two circles around the convex center of the attachment surface and a peripheral ring of fascicles of long filaments alternating with short hook-shaped filaments. The parasite cortex is a three-membrane pellicle with a well-developed dense fibrous glycocalyx and micropores characteristic of apicomplexans. Outside the attachment base, the parasite surface is organized into weakly expressed broad folds with shallow grooves between them. The pellicle between the grooves is lined by longitudinal ribbons of subpellicular filaments ending near the attachment fascicles of filaments. The micropores are located at the bottom of the grooves as well as on the attachment surface. The parasites do not form a direct contact with the host cell. The internal space of the parasitophorous sac is mostly translucent and continuous around the entire parasite, including the attachment site. The host-derived parasitophorous sac provides the parasites with permanent protection in the potentially unfriendly environment of the host intestine. These data interconnect the parasitophorous niche of *E. duboscqi* with that of *Cryptosporidium* [10–12].

In this paper, we describe a new species, *E. planoratum*, parasitizing in the intestine of the polychaete *Naineris quadricuspida*, compare the fine morphology of *E. planoratum* with that of the species *E. duboscqi*, and correct the diagnosis of the genus *Eleutheroschizon* based on the features of localization of protococcidians in the host. We also present concatenated DNA sequences of the nuclear ribosomal operon (SSU rDNA, ITS1, 5.8S rDNA, ITS2, and LSU rDNA) as well as the generated secondary structures of the ITS2 molecule of *E. duboscqi* and *E. planoratum*. The resulting phylogeny of sporozoans demonstrates the related position of *Eleutheroschizon* to Eimeriidae clade within Coccidiomorpha and the sisterhood of *Cryptosporidium* to gregarines. We discuss a new type of endoparasitism among sporozoans—parasitism in a closed epicellular niche, which has evolved convergently in *Eleutheroschizon* and *Cryptosporidium*.

2. Materials and Methods

2.1. Collection of Polychaete Hosts and Isolation of Parasites

Polychaetes *Scoloplos armiger* (Müller, 1776) (Orbiniidae, Polychaeta) were collected in the summer of 2014–2017 in the silty-sandy littoral zone of the mainland (66°33.200' N,

33°6.283' E) near N. A. Pertzov White Sea Biological Station of M. V. Lomonosov Moscow State University (WSBS), and in summer 2015 and 2018 in the silty-sandy intertidal zone of Bolshoy Goreliy Island (66°18.770' N; 33°37.715' E), Keret Archipelago, near the Educational and Research Station “Belomorskaia” of Saint-Petersburg University (ERS “Belomorskaia”; formerly the Marine Biological station). Both sampling sites are located in the Kandalaksha Bay of the White Sea.

Bristle worms *Naineris quadricuspida* (Fabricius, 1780) (Orbiniidae, Polychaeta) were collected in the summer of 2002–2018 in *Laminaria* kelp beds near Vichennaya Luda Island (66°19.615' N; 33°50.502' E), Keret Archipelago, Kandalaksha Bay, White Sea.

The examined animals were stored and dissected for the isolation of parasites according to Paskerova et al. [13].

2.2. Light Microscopy

Parasites attached to or separated from the host intestines were examined on living and/or squash preparations. The microscopes used for observation were a Leica DM2500 equipped with DIC optics, Plan-Apo objective lenses, a DFC 295 digital camera (Leica, Wetzlar, Germany) or Nikon DS-Fi3 (Nikon, Tokyo, Japan), Jenaval (Zeiss, Jena, Germany) equipped with an adapter and a Canon EOS 300D digital camera. The maximal dimensions of the parasite cells were measured using the ImageJ program (<https://imagej.net/ij/index.html>, accessed on 17 May 2023); the mean value (av.) and the standard error of the mean (SE) was calculated.

2.3. Electron Microscopy

For scanning (SEM) and transmission (TEM) electron microscopy, small pieces of polychaete intestine with attached parasites were fixed in 2.5% glutaraldehyde in 0.05 M cacodylate buffer (pH 7.4, and final osmolarity 720 mOsm) for 2 h, washed in filtered seawater or cacodylate buffer, and postfixed in 2% osmium tetroxide in the same buffer for 2 h. Fixation was performed at +4 °C. Fixed samples were dehydrated in an ascending ethanol series. For SEM, the fixed and dehydrated samples were dried at the critical point in liquid CO₂ and then coated with gold or platinum (20 nm). The samples were examined using GEMINI Zeiss Supra 40VP (Carl Zeiss, Jena, Germany), LEO 420 (Carl Zeiss, Jena, Germany) and/or Tescan Mira3 LMU (Brno, Czech Republic) scanning electron microscopes. For TEM, the samples, additionally dehydrated in ethanol/acetone mixture and rinsed in pure acetone, were embedded in EMBED epoxy resin (EMS). Ultrathin sections were stained according to standard protocols and examined using LEO 910 (Carl Zeiss, Jena, Germany), JEM-2100 (JEOL, Tokyo, Japan), and JEM-100B (JEOL, Tokyo, Japan) electron microscopes equipped with digital or film cameras.

2.4. Molecular Phylogenetic Analysis

To obtain DNA sequences, fragments of host tissue with attached parasites were placed in 30% alcohol. During the initial maceration of the prefixed host tissues (the first 15–20 min), parasites were knocked off the surface of the host intestinal epithelium using hand-drawn glass pipettes. This pretreatment partially preserved the parasitophorous sac around each parasite. Separated parasites were additionally washed in 30% alcohol and fixed in 96% alcohol. For DNA extraction, the following fixations were used: *E. duboscqi*–30 cells, WSBS, 2014, and *E. planoratum*–25 cells, ERS “Belomorskaia”, 2016.

DNA was extracted with the NucleoSpin Tissue kit (Macherey–Nagel GmbH & Co. KG, Düren, Germany). Whole genome amplification (WGA) was performed using the REPLI g Midi Kit (Qiagen, Manchester, UK). The rDNA fragments were amplified with the Encyclo PCR kit (Evrogen, Moscow, Russia) in a total volume of 20 µL in the following PCR steps: 95 °C for 2.5 min (initial denaturation); 40 cycles of 95 °C for 30 s (denaturation); 48–55 °C (depending on primers) for 30 s (annealing); 72 °C for 1.5 min (elongation); and 72 °C for 10 min (final extension). For *E. planoratum* sp. nov. ex *N. quadricuspida*, the following pairs of forward and reverse primers were used: 5'-TMYCYGRTTGATYCTGYC-3' and

5'-GGAAACCTTGTTACGACTTCTC-3' for 18S rDNA; 5'-GTACACACCGCCCGTCGCTC-3' and 5'-GACTCCTTGGTCCGTGTTTCAAGACG-3' for ITS1, ITS2, and 5.8S rDNA; and 5'-GTGACGATCTTCCTAGGATG-3' and 5'-MRGGCTKAATCTCARYRGATCG-3' for 28S rDNA. For *E. duboscqi* ex *S. armiger* the following were used: 5'-GTATCTGGTTGATCCTGCC AGT-3' and 5'-GGAAACCTTGTTACGACTTCTC-3' for 18S rDNA; 5'-GGACTATTACAATT GCTTTTGC-3' and 5'-GACTCCTTGGTCCGTGTTTCAAGACG-3' for ITS1, ITS2, and 5.8S rDNA; and 5'-GAGACCTAAGGAGCTGAAAG-3' and 5'-MRGGCTKAATCTCARYRGATC G-3' for 28S rDNA.

The 5.8S and LSU rDNA of *Margolisiella islandica* Kristmundsson et al., 2011 and *Monocystis agilis* Stein, 1848 were assembled from the available transcriptomic data (SRR12197183 and SRR8980208).

Three rDNA (SSU, 5.8S, and LSU) alignments containing different alveolates were generated in MUSCLE 3.6 [14] under default parameters and then manually adjusted and concatenated with BioEdit 7.0.9.0 [15]; columns containing few nucleotides or hypervariable regions were removed. The dataset for phylogenetic inference was designed in order to display the phylogenetic diversity of coccidiomorph sporozoans (see [1]). The dataset included 37 OTUs consisting of concatenated SSU, 5.8S, and LSU rDNA sequences (4527 bp). The missing 5.8S and LSU rDNA data from several OTUs were replaced with "N".

Bayesian inference (BI) analysis was performed with MrBayes 3.2.7a utilizing the resources of the CIPRES web server [16,17]. The analysis was performed under the GTR+I+I model with 4 rating categories. The chain heating coefficient (temp) was set to 0.2. The inference was conducted using four independent runs of four MCMC, and a consensus tree was built with a 50% burn-in after 10 million generations. The average standard deviation of the split frequencies at the end of computations was 0.002135. ML analysis was performed with the IQ-TREE 2.1.2 using the GTR+I+G4+F model and 1000 nonparametric rapid bootstrap pseudoreplicates to estimate branch support [18,19].

The predicted secondary structures of ITS2 molecules of *Eleutheroschizon* spp. were manually generated and tested via MFOLD in the temperature of 5–37 °C under default parameters, except for the suboptimality percentage parameter which was chosen as 15 [20]. To prove that *E. duboscqi* and *E. planoratum* are different species, compensatory base changes (CBCs) in secondary ITS2 molecule structures were searched [21–24].

3. Results

3.1. *E. duboscqi* Brasil, 1906, Emend

The detailed morphology of *E. duboscqi* trophozoites and gamonts was described in 2015 by Valigurová et al. using modern microscopic methods [10]. Here, we supplement this description with statistical and morphometric data on the White Sea material to further refine the diagnosis of the species (Table 1, Taxonomic Summary; Figures S1 and S2).

Table 1. Diagnostic characters of *Eleutheroschizon* species.

Species/ Characteristics	<i>E. duboscqi</i> Brasil, 1906, Type Species	<i>E. duboscqi</i> ; Emended Description	<i>E. murmanicum</i> Awerintzew, 1908	<i>E. planoratum</i> sp. nov.
Host	<i>Scoloplos armiger</i> (Müller, 1776), <i>Protoaricia oerstedii</i> (Claparède, 1864) (former <i>Theostoma oerstedii</i> (Claparède, 1864))	<i>Scoloplos armiger</i> (Müller, 1776)	<i>Ophelia limacina</i> (Rathke, 1843)	<i>Naineris quadricuspida</i> (Fabricius, 1780)
Locality	Luc-sur-Mer, English Channel, East Atlantic (<i>S. armiger</i>); L'Étang de Thau, Mediterranean Sea (<i>P. oerstedii</i>)	Velikaja Salma strait (WSBS) and Bolshoy Goreliy (ERS), Kandalaksha Bay, White Sea	Strait Ekaterininskaya Gavan', Kola Bay, Barents Sea	Vichennaya Luda Isl, Keret Archipelago, Kandalaksha Bay, White Sea

Table 1. Cont.

Species/ Characteristics	<i>E. duboscqi</i> Brasil, 1906, Type Species	<i>E. duboscqi</i> ; Emended Description	<i>E. murmanicum</i> Awerintzew, 1908	<i>E. planoratum</i> sp. nov.
Localization in the host	at the end of the first third of the intestine, often in the ventral groove	throughout the midgut; attached to the intestinal epithelium or free in the intestine cavity	attached to the intestinal epithelium or free in the intestine cavity	throughout the mid- and hindgut; usually attached to the intestinal epithelium
Infection: extensity (percentage of infected hosts), intensity (number of parasites per host)	about 5%, abundant	about 11% (16 out of 146) at WSBS and 16% (4 out of 25) at ERS, few tens	not in each host, abundant	about 83% (100 out of 121), several to several dozen cells
Cell shape	elongated bell, widest part facing to the host epithelium	helmet or elongated bell, straight or slightly curved, widest part facing to the host intestine	wide low cone, widest part facing to the host intestine	barrel-shaped, straight or slightly curved, flattened anterior end facing to the host intestine
Cell size (width x height (av. \pm SE, dataset), μ m)	up to 30 in height	6.5–15 \times 8.5–27 \times (11 \pm 1.7 \times 15 \pm 3.3, n = 18)	up to 50–60 \times 25–38	6–24 \times 7–36 (15 \pm 3.2 \times 24 \pm 4.5, n = 100)
Number of grooves (av., (min-max, dataset))	--	usually 12 (10–13, n = 21)	--	usually 12 (9–12, n = 15)
Anterior end (attachment base)	wide, with 2 circles of rounded lobes ("denticles" in origin.)	roundish, \times 4.4–12.7 (9.7 \pm 2.2, n = 11) μ m in diameter, convex, with 1–2 circles of rounded lobes (up to about 20 in total) and 1 peripheral ring of fascicles of long filaments alternating with short hook-shaped filaments	wide, convex, with 1 peripheral ring of 12–20 conical lobes ("denticles" in origin.)	oval, 9–19 (14.5 \pm 2.6, n = 5) μ m in max. diameter, flat, with wavy contour and 1 peripheral ring of fascicles of filaments
Posterior end; "tail" (distal part of the parasitophorous sac)	rounded; with 1 "tail", conical, pointed, sometimes hooked or ended in a very small ball	rounded, sometimes with a depression at the apex; with 1 (rarely 2–3 or absent) "tail" (conical, pointed, sometimes hooked or ended in a very small ball)	rounded; without "tail"	rounded, sometimes with a depression at the apex; with or without 1 "tail" (conical, pointed, sometimes hooked)
Nucleus: number, shape, size (width x length (av. \pm SE, dataset), μ m), position in parasite cell	--	1 large, roundish, 3.9–8.1 \times 3.0–9.0 (5.8 \pm 1.3 \times 5.7 \pm 1.3, n = 10), located in the widest cell part (macrogamonts); several small, spherical, 1.2–1.7 \times 1.2–1.6 (\times 1.4 \pm 0.1, n = 20), evenly distributed throughout the cytoplasm (microgamonts)	1 large, oval, centrally located (macrogamonts); multiple small nuclei at the cell periphery and 1 irregular oval nuclear residue (microgamonts)	1 large, spherical, 4–11 \times 4–11 (\times 7 \pm 1.2, n = 57), located in the widest cell part (macrogamonts); several small, evenly distributed throughout the cytoplasm (microgamonts)
Nucleolus: quantity, shape, size (widthwise x lengthwise, av. \pm SE, dataset), μ m), position in nucleus	--	1 large, spherical, 1.5–3.0 \times 1.4–2.8 (2.4 \pm 0.5 \times 2.3 \pm 0.6, n = 5), eccentrically located (macrogamonts); several fragmented (microgamonts)	1 large, spherical, centrally located (macrogamonts)	1 large, oval, 2.8–4.4 \times 1.6–3.5 (3.5 \pm 0.5 \times 2.4 \pm 0.4, n = 10), eccentrically located (macrogamonts)

Table 1. Cont.

Species/ Characteristics	<i>E. duboscqi</i> Brasil, 1906, Type Species	<i>E. duboscqi</i> ; Emended Description	<i>E. murmanicum</i> Awerintzew, 1908	<i>E. planoratum</i> sp. nov.
Merogony	absent	absent	absent	absent
Sporozoites (width × length, μm)	2 × 5, pointed; the nucleus located in the apical end	--	similar to <i>E. duboscqi</i>	--
Oocyst	several fan-shaped clusters of sporozoites connected at one end to a residual body	--	--	--
Motility	immotile	immotile	--	immotile
Characteristic features	--	formation of a parasitophorous sac from fused outgrowths of the infected enterocyte	paired association of one- or multinuclear (2–3 nuclei) cells by expanded parts, lobes absent (syzygy?)	formation of a parasitophorous sac from fused outgrowths of the infected enterocyte
rDNA sequences	--	SSU, 5.8S, LSU rDNA, ITS1, ITS2	--	SSU, 5.8S, LSU rDNA, ITS1, ITS2
References	[8,9]	[10], this study	[25]	this study

Abbreviations: --, no data; ?, contradictory or vague description requiring verification; av., average (mean); SE, standard error of the mean. The validation of the scientific names was conducted in the World Register of Marine Species [26].

3.1.1. Occurrence

Parasites were detected in polychaetes *Scoloplos armiger* collected at two sites: WSBS and ERS “Belomorskaia” (see M and M; [10]). The prevalence (extensity) of parasitic infection at these sites differed slightly: 11% (16 out of 146) and 16% (4 out of 25) of infected polychaetes, respectively. Typically, the intensity of infection is a few tens of parasites per host. The parasites localize on the surface of the intestinal epithelium of the host midgut, usually close to the hindgut and often together with blastogregarines *Siedleckia nematoides* Caullery et Mesnil, 1898 [2]. In rare cases, individual parasites are free in the intestine cavity of the host.

3.1.2. Morphology

The examined parasites, isolated from polychaetes collected at different sampling sites in the White Sea, were identical in their morphology and fine structure. In a host, macrogamonts were about 10–15 times more numerous than microgamonts. Macrogamonts are distinguished by a large number of amylopectin granules, lipid droplets, and dense bodies that completely fill the parasite cytoplasm. Microgamonts are usually smaller than macrogamonts and are depleted in cytoplasmic inclusions. Each epicellularly localized parasite cell is covered by a two-membrane parasitophorous sac formed by the invaded host cell. See Table 1 and Figures S1 and S2 for other details.

The observed endogenous stages showed no cell motility.

3.2. *E. planoratum* sp. nov.

3.2.1. Occurrence

This protococcidian parasitizes the polychaetes *Naineris quadricuspida* from the White Sea. In total, 83% polychaetes were infected (100 out of 121). Attached and sometimes non-attached parasites of different sizes were found in the mid- and hindgut of the host. The intensity of infection usually ranged from single cells to several tens of parasites per host (Table 1, and Figures 1–3).

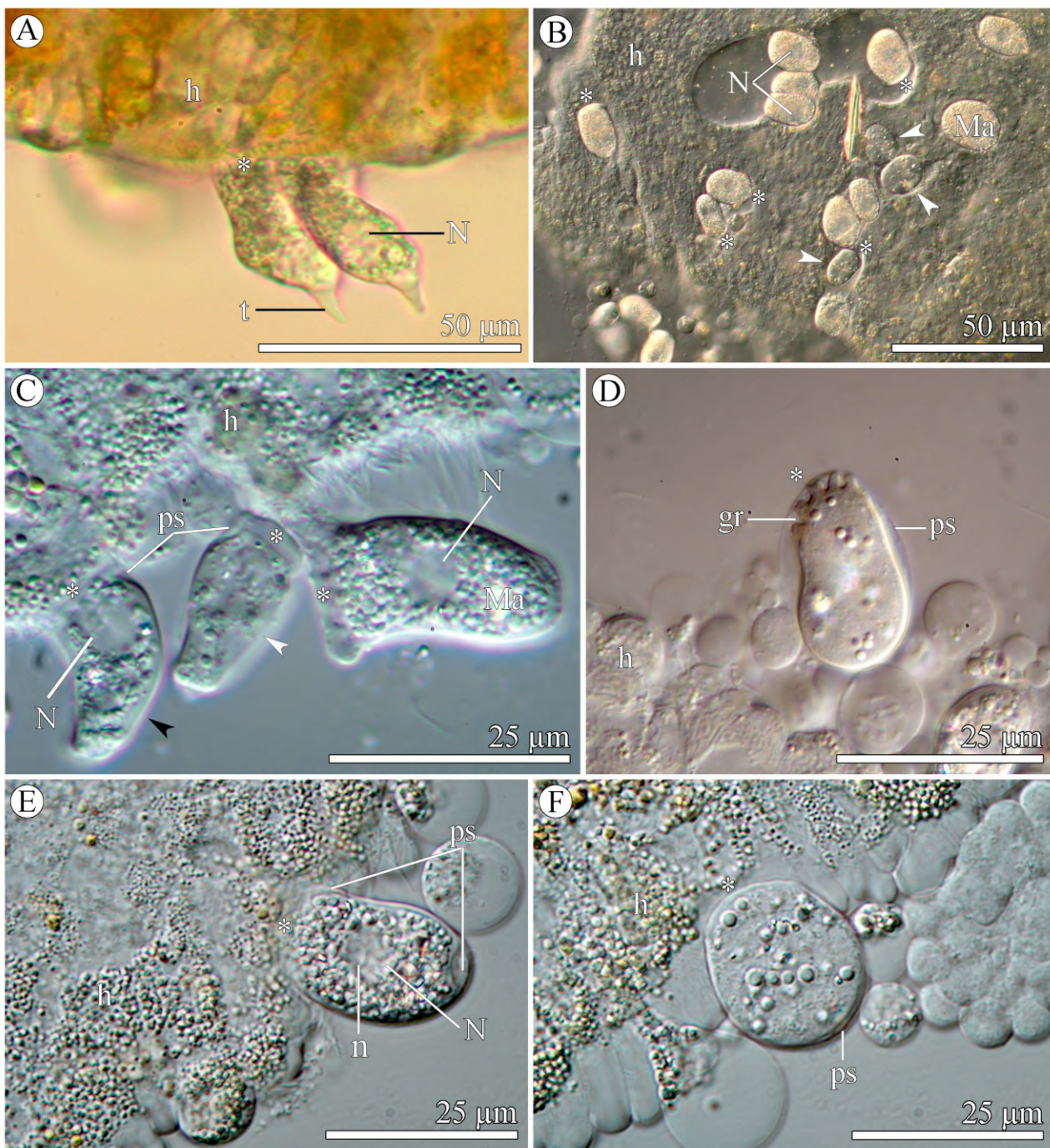


Figure 1. General morphology of *Eleutheroschizon planoratum* sp. nov. Bright field (A) and differential interference (B–F) light microscopy. (A) Two macrogamonts attached to the host intestinal epithelium. Live preparation. (B) Macrogamonts and microgamonts in the host intestinal epithelium. Squash preparation. (C) Gamonts slightly compressed. Squash preparation. (D) Microgamont, placed at an angle, partially showing folds that make the edge of the attachment site undulated. Squash preparation. (E,F) Macrogamont (E) and microgamont (F) slightly compressed. Squash preparations. Abbreviations: *, attachment base of the parasite; gr, groove on the parasite surface; h, host intestinal epithelium; Ma, macrogamont; N, nucleus; n, nucleolus; ps, parasitophorous sac; t, “tail”—caudal appendage of the parasitophorous sac; white arrowheads point to microgamonts; black arrowhead points to young macrogamont.

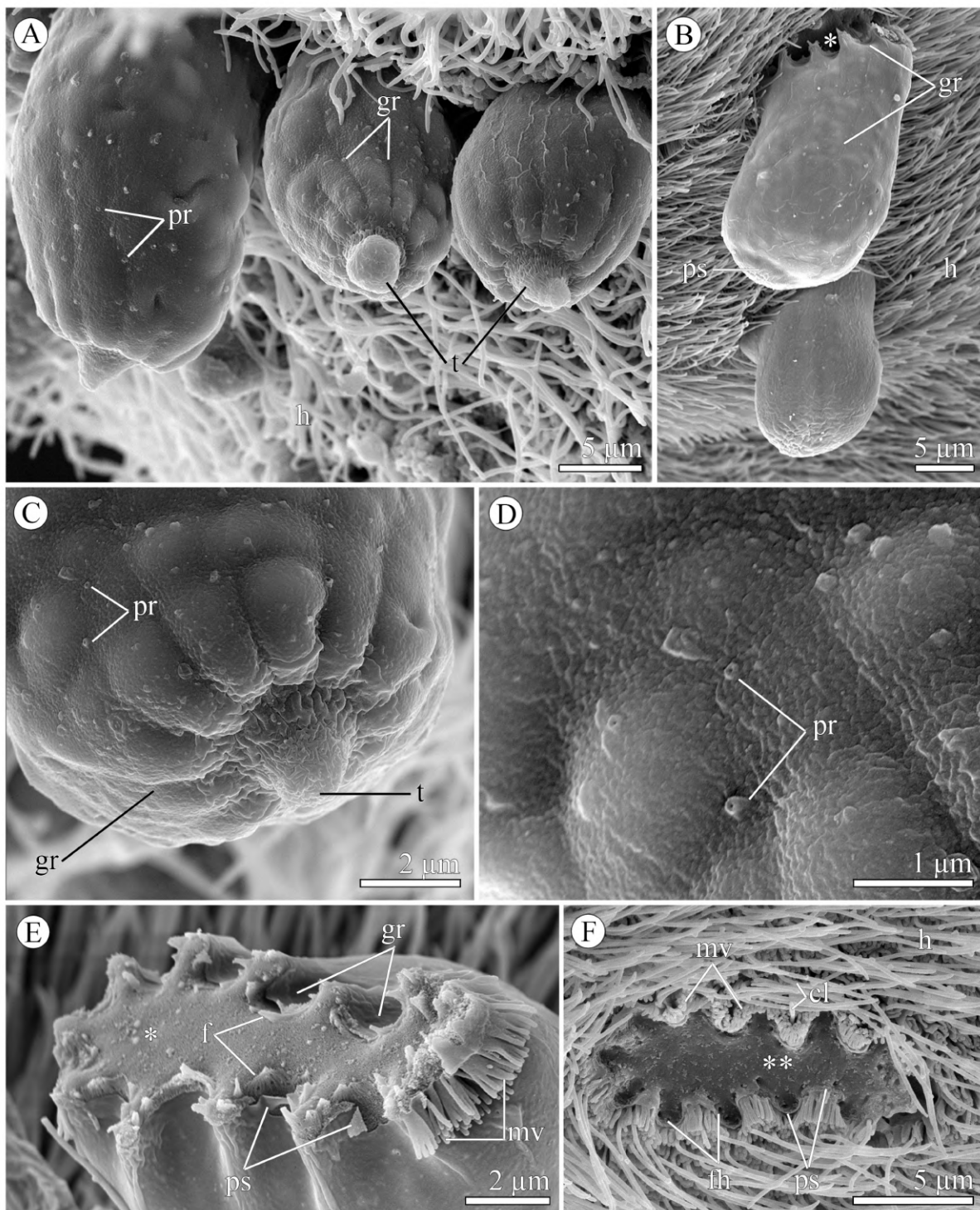


Figure 2. Fine structure of *Eleutheroschizon planoratum* sp. nov. Scanning electron microscopy. (A,B) Parasites attached to the host intestinal epithelium. (C) Posterior end of a parasite enveloped by the parasitophorous sac. (D) Higher magnification of pores visible in the parasitophorous sac (C). (E) Attachment site of a mechanically dislodged parasite. (F) Crater left on the host tissue after detachment of a parasite. Abbreviations: *, attachment base of the parasite; **, crater on the host intestinal epithelium, corresponding to the parasite attachment base; cl, cilia of the host intestinal epithelium; f, fascicle of filaments of the parasite attachment base; fh, hole for a fascicle of filaments; gr, groove on the parasite surface; h, host intestinal epithelium; mv, microvilli of the host enterocyte; pr, pores; ps, parasitophorous sac; t, “tail”—caudal appendage of the parasitophorous sac.

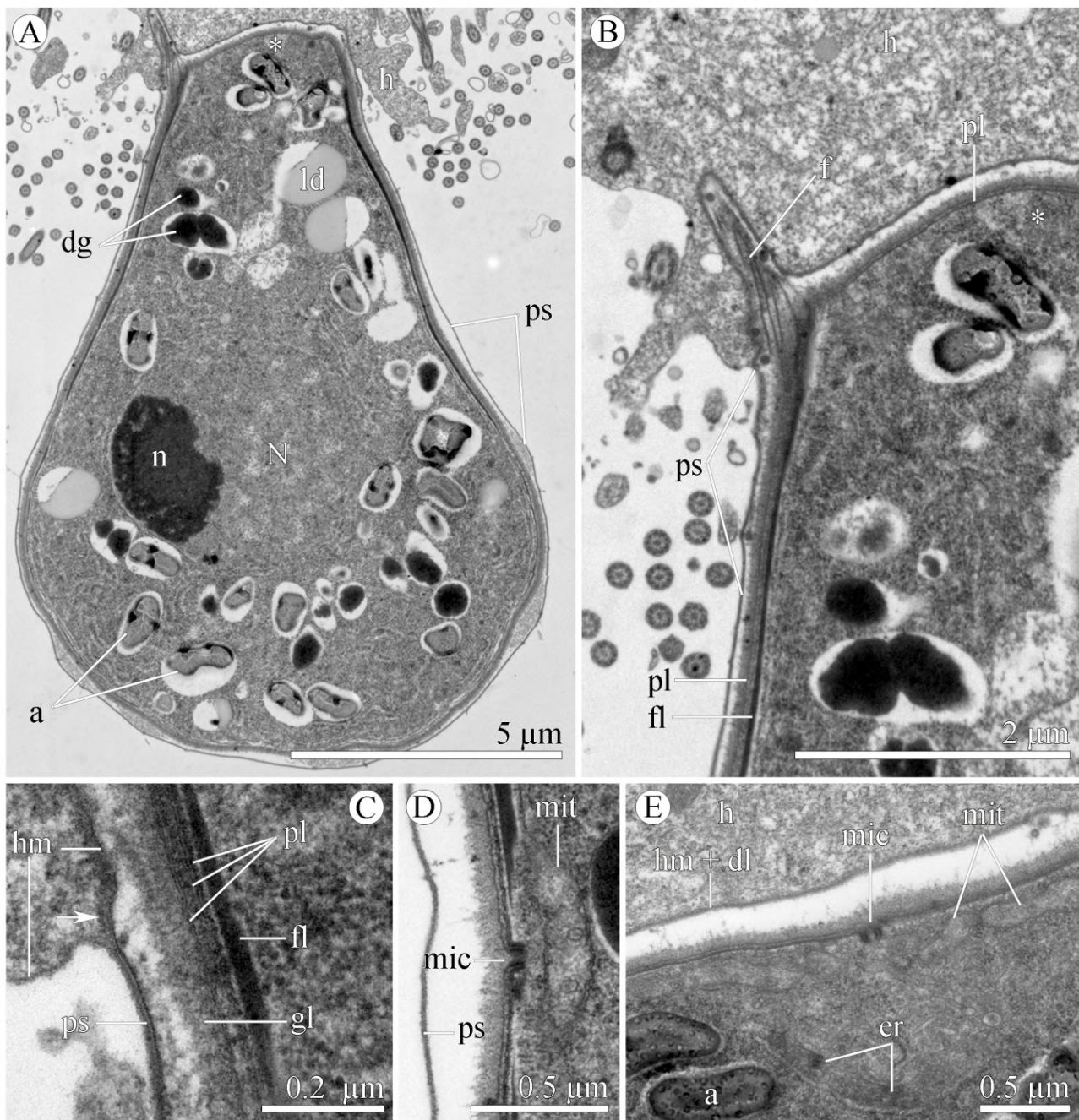


Figure 3. Fine structure of *Eleutherschizon planoratum* sp. nov. Transmission electron microscopy; longitudinal sections. (A) General view of an attached macrogamont. (B) Details of the parasite attachment base. Part of A at higher magnification. (C) Details of the parasitophorous sac. (D) Details of the parasite cortex out of the attachment site. (E) Details of the attachment site. Abbreviations: *, attachment base of the parasite; a, amylopectin granule; dl, electron-dense line of filaments under the host cell membrane; dg, dense granule; er, endoplasmic reticulum; f, fascicle of filaments of the parasite attachment base; fl, subpellicular filaments of the parasite; gl, glycocalyx; gr, groove on the parasite surface; h, host intestinal epithelium; hm, host cell membrane; ld, lipid droplet; mic, parasite micropore; mit, parasite mitochondrion; N, nucleus; n, nucleolus; pl, pellicle; ps, parasitophorous sac; white arrow points to an electron-dense line of filaments under the host membrane in the site of parasite–host cell contact.

3.2.2. Morphology

Protococcidians are barrel-shaped, straight or slightly curved. Their oval, flat attachment base faces to the host intestinal epithelium. The posterior end facing the intestine lumen is rounded, sometimes with a depression at the apex (Figure 1A). Parasites vary from 7 to 36 μm in length and from 6 to 24 μm in width. The ratio of microgamonts to macrogamonts is approximately one to five (Figure 1B). Macrogamonts are slightly larger than microgamonts. They have many amylopectin granules and lipid droplets, as well as one large nucleus located in the widest part of the cell, usually near the parasite attachment base. An irregularly shaped nucleolus is located eccentrically in the nucleus. Microgamonts have several small nuclei evenly distributed throughout their optically light cytoplasm having a few inclusions (Figure 1C–F).

Like in *E. duboscqi*, the entire cortex of *E. planoratum* is organized as a three-membrane pellicle covered with fibrous glycocalyx. The parasite surface bears alternating broad folds and shallow grooves which extend to the flat base, creating a wavy contour of the attachment surface. Fascicles of filaments are located along the wavy periphery of the attachment site (Figures 1D, 2 and 3A,B). Craters left after detached parasites are flat and have only a peripheral ring of holes corresponding to fascicles of filaments (Figure 2F). The number of grooves varies from 9 to 12 (usually 12). Their cortex is additionally lined by longitudinal ribbons of subpellicular filaments terminating near the fascicles of filaments of the attachment base. Micropores are located at the bottom of grooves and on the attachment surface. The cytoplasm beneath the cortex contains mitochondria, vesicles, and membranes of endoplasmic reticulum, usually clustered near micropores (Figure 3C–E). Unlike *E. duboscqi*, *E. planoratum* does not have any outgrowths on the attachment surface of the flat base.

Similar to *E. duboscqi*, *E. planoratum* is surrounded by a host cell-derived, two-membrane parasitophorous sac usually forming a caudal appendage, the “tail”. “Tails” are conical, pointed, and sometimes slightly hooked (Figure 1A,C–F and Figure 2A–C). There are pores in the parasitophorous sac (Figure 2C,D). The internal space of the parasitophorous sac is translucent and clearly visible between the parasite attachment site and the apical surface of the host cell, as there is no direct contact between the two cells (Figure 3). The host cell membrane in the site of *E. planoratum* attachment is reinforced by an electron-dense line of fibrillar-like appearance (Figure 3C).

The observed endogenous stages were immotile.

3.2.3. Phylogenetic Position of *Eleutheroschizon* spp.

We obtained nearly complete rRNA operon sequences (SSU rDNA, ITS1, 5.8S rDNA, ITS2 and LSU rDNA) for *E. duboscqi* (5775 bp) and *E. planoratum* sp. nov. (5746 bp) and performed two phylogenetic analyses, Bayesian (BI, Figure 4) and Maximum Likelihood (ML, not shown). Both analyses showed completely identical tree topologies.

The analyses show monophyly of the major coccidiomorph groups: eimeriid and adeleid coccidians, corallicolids, lineages of haematozoans, and marosporids (eococcidians). The newly sequenced *Eleutheroschizon* species form a strongly supported monophyletic group (posterior probability, PP = 1; and bootstrap percentage, BP = 100) together with environmental sequences obtained from intertidal marine sediment collected in Greenland. This group subdivides into two robust clades: a clade where *E. duboscqi* with one uncultivated Greenlandic eukaryote branches off from *E. planoratum* with another uncultivated Greenlandic eukaryote (PP = 1, and BP = 98), and a clade of three uncultivated Greenlandic eukaryotes (PP = 1, and BP = 100). The combined clade of protococcidians, *Eleutheroschizon* spp. and environmental sequences, appears as a sister to the clade of eimeriid coccidians, corallicolids, and a parasite from the sea cucumber *Apostichopus japonicus* (Selenka, 1867), although with insufficient evidence (PP = 0.77, and BP = 41). Outside the Coccidiomorpha clade, *Cryptosporidium* is a sister to gregarines with strong support (PP = 1.0, and PB = 100).

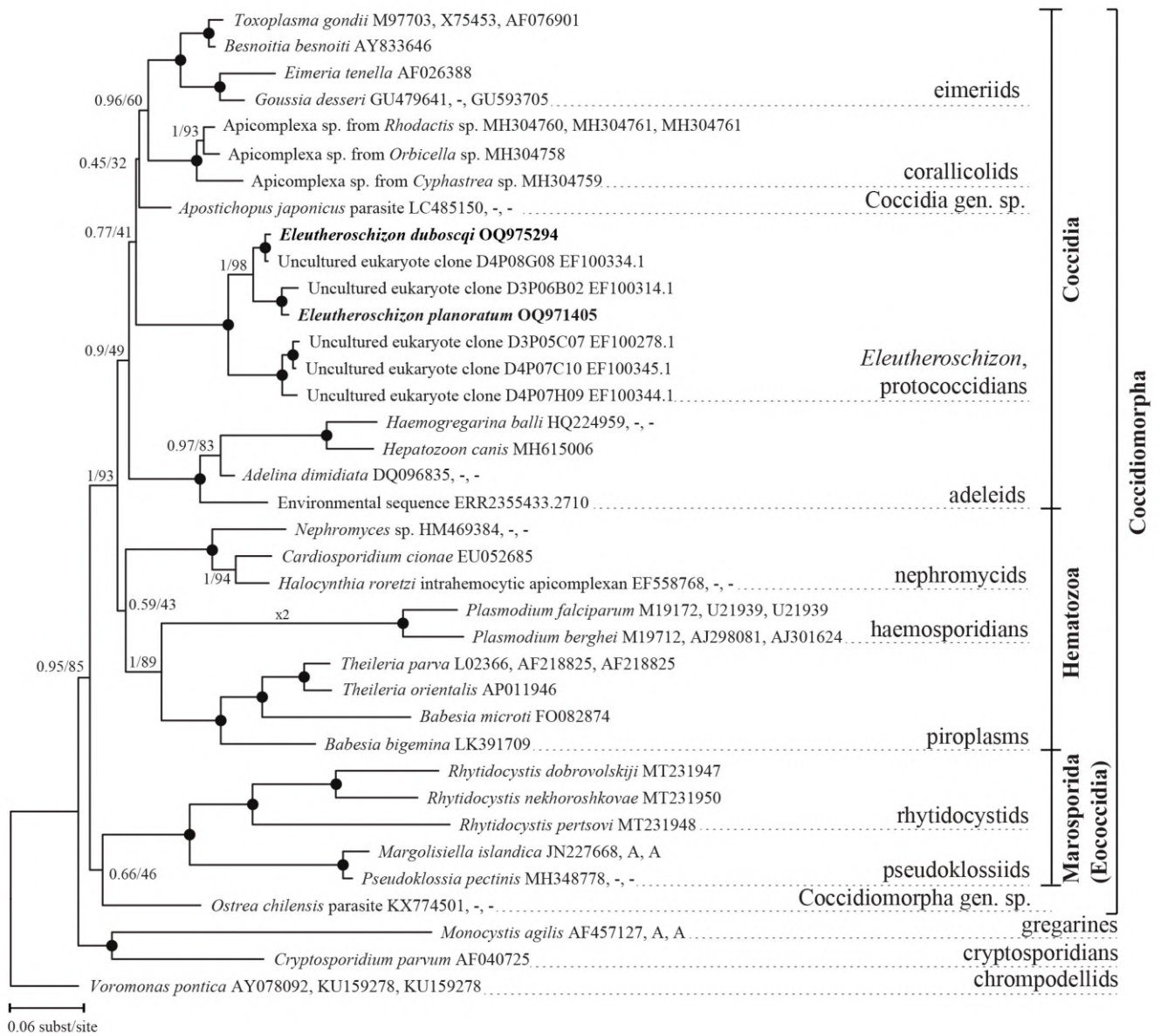


Figure 4. Bayesian tree of coccidiomorphs inferred from the dataset of 37 concatenated SSU, 5.8S, and LSU rDNA sequences (4527 bp) under the GTR+ Γ +I model with 4 rate categories. Numbers at branches indicate Bayesian posterior probabilities (numerator) and ML bootstrap percentage (denominator). Black dots on the branches indicate Bayesian posterior probabilities and bootstrap percentages of 1.0 and 100%, respectively. The newly obtained sequences of *Eleutheroschizon duboscqi* and *E. planoratum* are in bold. The names of major coccidiomorph lineages correspond to Janouškovec et al., 2019, Mathur et al., 2020, and Miroljubova et al., 2020 [1,5,27].

We mapped the complementary regions of 5.8S rRNA and LSU rRNA and thus localized the ITS2 region (Figure S3). Like some gregarines [28], *Eleutheroschizon* spp. have only three helices in the secondary structure of their ITS2 molecules. The first helix differs in the two species in the number of nucleotides. Based on the similar nucleotide motif in both species, we localized the target site of the expansion in the inner loop, resulting in the unusual branched helix I in *E. planoratum* (Figure S4). The second helix has the typical U-U mismatch [29]. The third helix is the longest and most variable; close values of initial ΔG were calculated for alternative folds of helix III. We chose variants with a similar arrangement of the conserved motif (Figure S4), but this choice suggests independent nucleotide extensions in the helix III in the two *Eleutheroschizon* species. Helix III seems

to be partially unpaired due to the large number of mismatches and the small number of strong G-C pairs. Two CBCs were found in both *Eleutheroschizon* spp.: one in helix I and one in helix II (Figure 5). Considering only the most conserved part, one or two more CBCs are likely in helix III.

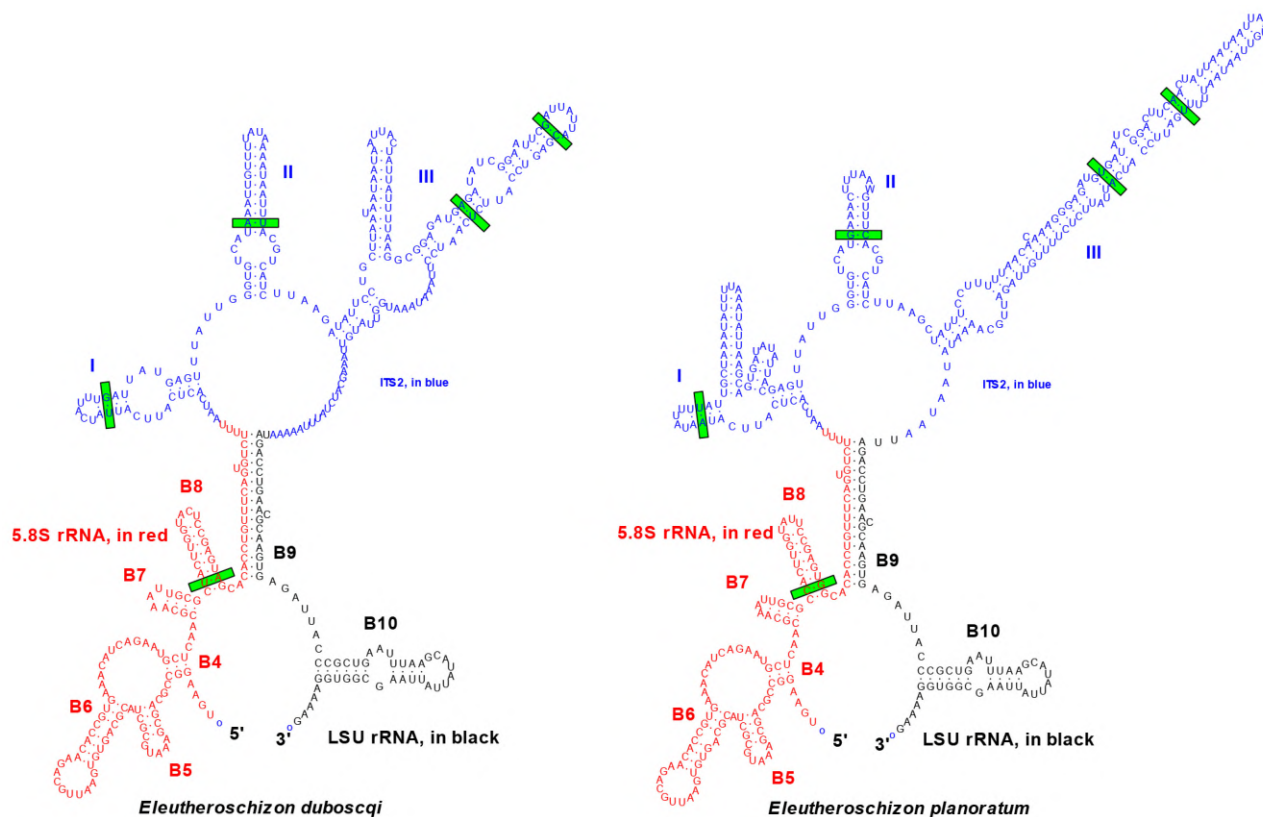


Figure 5. Predicted secondary structures of ITS2 transcripts of *Eleutheroschizon duboscqi* and *E. planoratum* demonstrating differences between them. Helices are numbered I–III. Nucleotides involved in compensatory base changes are highlighted in green.

4. Discussion

4.1. Justification of Species

There are currently two known species of protococcidians, *E. duboscqi* and *E. murmanicum*. *E. duboscqi* was first described by L. Brasil [8] from *Scoloplos armiger* (Orbiniidae) collected in the English Channel using light microscopy. The life cycle of this parasite was interpreted in a study of protococcidian-infected polychaetes *Protoarcia oerstedii* (Orbiniidae) from the Mediterranean Sea [9]. The sequential epicellular development of trophozoites and gamonts of the parasite in the gut of *S. armiger* was demonstrated on materials from the White Sea [10]. Only materials from the White Sea have molecular evidence for this parasite [1]. In all studies, after the work of Brasil [8], it was assumed that the studied parasites, although collected in different locations, were *E. duboscqi* because of their morphological similarity to the first description. We adhere to this assumption because verification that this particular species, and no other related species, occurred in all the named sites is not possible at this time. We summarized previously published old light [8,9], modern light and electron [10] microscopic observations and added new information on the occurrence and morphometry of *E. duboscqi* (Table 1).

E. murmanicum was described as an extracellular intestinal parasite of the polychaete *Ophelia limacina* (Opheliidae) collected in the Barents Sea [25]. Like *E. duboscqi*, *E. murmanicum* attaches to the host enterocyte using a complex attachment apparatus. The attachment surface is wide, convex, with 12–20 conical lobes arranged in one periphery circle (Table 1).

The protococcidian described in this study is parasitic in the intestine of the polychaete *N. quadricuspida* (Orbiniidae). In cell morphometry, it is larger than *E. duboscqi*, but smaller than *E. murmanicum*. This parasite has a flat attachment surface without any lobes. Based on these characteristics, we consider it as a new species, *Eleutherschizon planoratum* sp. nov. (Table 1, Taxonomic Summary). This conclusion is also supported by phylogenetic analyses conducted using concatenated nuclear ribosomal operon DNA sequences (SSU rDNA, ITS1, 5.8S rDNA, ITS2, and LSU rDNA) and compensatory base changes in secondary ITS2 molecule structures of *E. duboscqi* and *E. planoratum* (Figures 4 and 5).

Based on the surface morphology and fine structure of *E. duboscqi* and *E. planoratum* as well as the parasitophorous sac formed by the host cell around them, we emend the diagnosis of the genus *Eleutherschizon* and the species *E. duboscqi* (Taxonomic Summary).

4.2. Localization in a Closed Epicellular Niche

Representatives of the family Eleutherschizonidae are characterized by epicellular localization and distinct cell polarity, the absence of schizogony (merogony) and the presence of extracellular gamogony in their life cycle, and the characteristic structure of oocysts [9]. Both *E. duboscqi* and *E. planoratum* are epicellular in relation to the host cell and are surrounded by the so-called parasitophorous sac ([10], this study). Using (immune) fluorescent labelling for confocal microscopy, it has been shown that filamentous actin and myosin as well as polymerized α -tubulin are present in the wall of parasitophorous sac built around *E. duboscqi* [10]. These observations confirm the inclusion of microvilli and cilia of the invaded host enterocyte in the formation of the parasitophorous sac around the parasite.

The localization of protococcidians is comparable to that of *Cryptosporidium* ([11,12,30–33], etc.). The parasitophorous sac around *Eleutherschizon* and *Cryptosporidium* is a closed epicellular niche for development of the parasite, which, on one hand, protects the parasite from the aggressive internal environment and immune system of the host and, on the other hand, helps the parasite communicate with the environment through the pores ([10–12,34], this study).

Cryptosporidians and protococcidians differ in the way they attach to the host cell. *Cryptosporidium* are true epicellular parasites that form a Y-shaped annular contact with the host cell membrane. Their feeding organelle, developed from an anterior vacuole of the sporozoite, directly faces the cytoplasm of the host cell in its apical part, which is modified by the parasite and separated from the rest of the host cell cytoplasm by a dense band rich in actin [10,35,36]. Cryptosporidians appear to obtain nutrients from the host cell via myzocytosis using their feeding organelle [11,12,31,32,34,37–41]. Protococcidians develop an attachment organelle, which is most likely formed not so much from the sporozoite apex, with which the organelles of the apical complex in all sporozoans are physiologically connected, as from the entire anterior part of the parasite cell facing the host enterocyte. Therefore, it cannot be compared to either the archigregarine mucron or the eugregarine epimerite [28,42]. In contrast to gregarines and cryptosporidians, protococcidians do not form tight contacts with the host cell membrane, at least at their trophozoite and gamont stages ([10], this study). Feeding via myzocytosis does not seem to be characteristic of this parasite, which is devoid of the organelles of the apical complex at these stages. Numerous micropores, often associated with vesicles, mitochondria, and membranes of endoplasmic reticulum, are located both at the bottom of the superficial grooves and on the attachment surface of *Eleutherschizon* parasites. This may indicate that some transport of substances from the internal space of the parasitophorous sac to the parasite cytoplasm can be mediated by its pellicle and micropores [43–45].

E. duboscqi probably forms a tight contact with the host cell only at the stage of sporozoite–host cell interaction. As soon as the process of parasitophorous sac formation is initiated (and this process apparently occurs faster than in *Cryptosporidium*), the parasite loses this presumably direct contact with the host cell membrane and begins to form an attachment apparatus (see Figure 2A in [10]). The role of this apparatus is most likely reduced

to lead to an increase in the attachment surface for the adhesion of the parasite to the host cell and for the transport of substances from the internal space of the parasitophorous sac into the cytoplasm of the protococcidian. It should be added that there is ample evidence that *Cryptosporidium* remotely induces apical surface changes not only in the target cell but also in the neighboring host cells [10–12,30,32,34,46]. Collectively, *Eleutheroschizon* spp. can be considered as hemiepicellular parasites that remotely affect the apical part of the host cell during most of the endogenous phase of their life cycle.

For all sporozoans, the involvement of the organelles of the apical complex (conoid, rhoptries, and micronemes) of sporozoites in search for, attachment to, and interaction with the host cell is obvious [47]. The nuances of the interaction between the parasite and the host cell are determined by the variety of secretions produced by sporozoans. Sporozoans initiate the formation of a closed parasitophorous niche (parasitophorous vacuole or parasitophorous sac) at the expense of the host cell using its various cellular mechanisms. We expect that the mechanisms of the host cell response to *Eleutheroschizon* parasitism will be similar to those of *Cryptosporidium* action. In both cases, the host cell builds protrusions on its apical surface with further fusion. For this process, the host molecular mechanisms to remodel actin and increase local cell volume must be induced by the parasite activation of different signaling pathways in the host membrane ([39] and references therein). A dense band of microfilaments under the host cell membrane at the site of parasite attachment is also one of the host cell responses to the action of these parasites [36]. We also assume that transporters in the target cell membrane may be modified by an epicellularly developing *Eleutheroschizon* to maximize the uptake of key substrates to meet their metabolic needs as demonstrated in the case of *Cryptosporidium* parasitism [44].

4.3. Parasitism in a Closed Epicellular Niche Evolved Converently

The discovery of the sisterhood of *Eleutheroschizon* and eimeriid coccidians was first made using multiprotein phylogeny and supported in later works with multigene phylogenies [1,5–7]. Despite the low supports, the overall topology of our rDNA phylogeny is consistent with the multimarker phylogenies. Sequences of other protococcidians whose composition, judging from morphological descriptions [4], is highly diversified are not available to date. Our phylogenetic data additionally show the formation of a clade in which two lineages are distinguished, the genus *Eleutheroschizon* and an additional new clade of a genus or higher level combining uncultivated eukaryotes from the Greenland intertidal zone [48]. The possible affinity of *Cryptosporidium* to gregarines was first shown in 1999 [49]. In recent phylogenetic works, *Cryptosporidium* occupies an inconsistent position in topologies: at the base of Coccidiomorpha, as a sister group to Gregarinomorpha, or as a basal group to all sporozoans, but always with moderate support [1,6,7,27,50,51]. In the present study, *Cryptosporidium* shows strong affinities with gregarines. To summarize, *Eleutheroschizon* and *Cryptosporidium* are phylogenetically distant sporozoans.

Comparative morphological data on the localization of *Eleutheroschizon* and *Cryptosporidium* together with phylogenetic reconstructions strongly suggest an independent origin of parasitism in a closed epicellular niche. The convergent development of such a niche is probably due to parasites' induction of the same host cellular mechanisms.

4.4. Taxonomic Summary

Phylum Apicomplexa Levine, 1970
Subphylum Sporozoa Leuckart, 1879
Class Coccidiomorpha Doflein, 1901
Order Protococcidiida Kheisin, 1956
Family Eleutheroschizonidae Chatton and Villeneuve, 1936
Genus *Eleutheroschizon* Brasil, 1906, emend.

Emended diagnosis. Trophozoites and gamonts epicellular covered the host-derived two-membrane parasitophorous sac, usually forming a caudal appendage ("tail"). Anterior

end transformed into the attachment apparatus. Posterior end rounded or had a depression at the apex. Cell surface with shallow grooves extended to the attachment base. Three-membrane pellicle additionally lined by longitudinal ribbons of subpellicular filaments, located between grooves and terminated near the attachment base. Micropores typical to sporozoans located at the bottom of grooves and on the attachment surface. Macrogamonts filled with more inclusions, usually larger, and occur more frequently than microgamonts. Oocysts with several fan-shaped clusters of sporozoites connected at one end to a residual body. Endogenous stages immotile. Intestine of polychaetes.

Type species. *Eleutheroschizon duboscqi* Brasil, 1906.

Remarks. Three named species.

Eleutheroschizon duboscqi Brasil, 1906, emend.

Emended diagnosis. Characteristics of the genus. Parasites helmet-shaped or elongated barrel-shaped, sometimes slightly curved; 6.5–15 µm long, 8.5–27 µm wide. The attachment base convex, with 1–2 circles of rounded lobes and 1 peripheral ring of fascicles of long filaments alternating with short hook-shaped filaments. Shallow grooves 9–12 (usually 12). Nucleus of macrogamonts roundish, 3.9–8.1 × 3.0–9.0 µm, located in the widest cell part, with one large, spherical, nucleolus, 1.5–3.0 × 1.4–2.8 µm, eccentrically located. Nuclei of microgamonts spherical, 1.2–1.7 × 1.2–1.6 µm, evenly distributed throughout the cytoplasm, with fragmented nucleoli.

Hosts and localities. Bristle worms *Scoloplos armiger* (type host). Luc-sur-Mer, English Channel, East Atlantic (type locality). *Protoaricia oerstedii* (Orbiniidae, Polychaeta), Mediterranean Sea.

Localization in the host. Intestine (midgut and hindgut).

Host and localities used in emended diagnosis. Bristle worms *Scoloplos armiger* (Orbiniidae, Polychaeta). Velikaja Salma strait (66°33.200' N, 33°6.283' E) and Bolshoy Goreliy Island of Keret Archipelago (66°18.770' N; 33°37.715' E), Kandalaksha Bay, White Sea.

Material for emended diagnosis. SEM stubs, resin blocks and fixed slides containing parasites and pieces of infected host intestine deposited in the collection of the Department of Invertebrate Zoology, St Petersburg University. Figures S1 and S2 (this publication) show some of the syntypes.

DNA sequences. SSU, 5.8S, and LSU rDNA, ITS1, ITS2 sequences for individuals, isolated from the polychaetes *Scoloplos armiger* (WSBS, White Sea) (GenBank OQ975294, SRX6640465).

Remarks. The original spelling of the species name is “*duboscqi*”, given in honor of the French marine biologist and parasitologist Octave Duboscq.

Eleutheroschizon planoratum sp. nov.

Diagnosis. Characteristics of the genus. Parasites barrel-shaped, straight or slightly curved; 7–36 µm long, 6–24 µm wide. Attachment base flat with wavy contour and 1 peripheral ring of fascicles of filaments. Shallow grooves 10–13 (usually 12). Nucleus of macrogamonts roundish, 3.9–8.1 × 3.0–9.0, located in the widest cell part. Nuclei of microgamonts small, spherical, 1.2–1.7 × 1.2–1.6, evenly distributed throughout the cytoplasm.

Type material. SEM stubs, resin blocks, and fixed slides containing parasites and pieces of infected host intestine deposited in the collection of the Department of Invertebrate Zoology, St Petersburg University (numbers 550-551_001–550-551_030, the type specimen-550-551_006). In this publication, Figure 2E is the iconotype; rest of the images demonstrate syntypes.

Type host and locality. Bristle worms *Naineris quadricuspida* (Orbiniidae, Polychaeta). Vichennaya Luda Island of Keret Archipelago (66°19.615' N; 33°50.502' E), Kandalaksha Bay, White Sea.

Localization in the host. Intestine (midgut and hindgut).

DNA sequences. SSU, 5.8S, and LSU rDNA, ITS1, ITS2 sequences for individuals, isolated from the polychaetes *Naineris quadricuspida* (White Sea) (GenBank OQ971405).

Etymology. The species name, *planoratum*, refers to the flat anterior end of the proto-coccidian and is derived from the Latin adjective “*planus*” (flat) and noun “*os*” (mouth).

ZooBank number of publication.

LSID urn:lsid:zoobank.org:pub:C78403C8-A93F-4871-B306-BDE05DFB59DA.

ZooBank number of new species.

LCID: urn:lsid:zoobank.org:act:28CB87BF-7E0C-4CE5-97A2-053411F825DA.

5. Conclusions

The study of localization of protococcidians in the host sheds light on the diversification of host–parasite interactions in Sporozoa (Apicomplexa). Comparison of the formation and structure of the parasitophorous niche formed around phylogenetically distant sporozoans *Eleutheroschizon* and *Cryptosporidium* indicates an independent origin and convergent evolution of the closed epicellular parasitism—development of the parasite in a closed epicellular niche formed by the invaded host cell.

Supplementary Materials: The following supporting information can be downloaded at: <https://www.mdpi.com/article/10.3390/d15070863/s1>. Figure S1. General morphology of *Eleutheroschizon duboscqi* ex *Scoloplos armiger* from the White Sea. Light differential interference (A–C), fluorescence (C) and bright field (D–F) microscopy. (A) Macro- and microgamonts attached to the host intestinal epithelium. Squash preparation. (B) Macrogamont. Squash preparation. (C) Microgamont with several nuclei. Squash preparation (left part), fluorescent staining of nuclei with DAPI (right part). (D) Detached gamont in the lumen of host intestine. Histological section, staining with hematoxylin after Boehmer. (E,F) Attached macrogamont (E) and microgamont (F). Semithin sections, staining with toluidine blue. Abbreviations: *, site of parasite attachment; dg, dense granule; Ed, *E. duboscqi*; h, host intestinal epithelium; ld, lipid droplet; N, nucleus; n, nucleolus; ps, parasitophorous sac surrounding the parasite; Sn, blastogregarine *Siedleckia nematoides* co-parasitizing the host intestine; t, “tail”—a caudal appendage of the parasitophorous sac; black arrowheads point to macrogamonts; white arrowheads point to microgamonts. Figure S2. Fine structure of *Eleutheroschizon duboscqi* ex *Scoloplos armiger* from the White Sea. Scanning (A–F) and transmission (G–I) electron microscopy. (A,B) Attached gamonts. (C) Higher magnification of the part B (frame) showing a rupture of the parasitophorous sac and exposure of the parasite surface. (D,E) Craters left on the host tissue after parasite detachment: young (D) and mature (E) gamonts. (F) Mature parasite slightly detached from the host epithelium and showing details of the attachment site. (G,H) Attached macrogamont (G) and microgamont (H). Longitudinal ultrathin sections. (I) Details of organization of the parasite attachment base and of the parasitophorous sac at a higher magnification. Longitudinal ultrathin section. Abbreviations: *, surface of the parasite attachment site; **, crater on the host intestinal epithelium, correspondent to the parasite attachment surface; a, amylopectin granule; dl, electron-dense line of filaments under the host cell membrane; dg, dense granule; f, fascicle of filaments of the parasite attachment base; fh, hole for a fascicle of filaments; fl, subpellicular filaments of the parasite; gl, glycocalyx; gr, groove on the parasite surface; h, host intestinal epithelium; hm, host cell membrane; hmit, host mitochondrion; l, lobe of the parasite attachment site; lh, hole for a lobe; ld, lipid droplet; mic, parasite micropore; mit, parasite mitochondrion; N, nucleus; p, parasite surface exposed in the parasitophorous sac rupture; pr, pore in the parasitophorous sac; ps, parasitophorous sac (G–I) or site of the parasitophorous sac detachment (E,F); t, “tail”—caudal appendage of the parasitophorous sac; white arrowheads limit the parasite trimembrane pellicle. Figure S3. Predicted secondary structure of ITS2 and B domain of LSU rRNA in *Eleutheroschizon duboscqi* and *E. planoratum* sp. nov. Figure S4. Conservative nucleotide motifs in helix I (in blue) and helix III (in magenta) of ITS2 in *Eleutheroschizon duboscqi* and *E. planoratum* sp. nov.

Author Contributions: Conceptualization, G.G.P. and T.G.S.; formal analysis, all authors; investigation, all authors; data curation, all authors; writing—original draft preparation, G.G.P. and T.S.M.; writing—review and editing, all authors; visualization, all authors. All authors have read and agreed to the published version of the manuscript.

Funding: This research was funded by Russian Science Foundation, grant number 22-24-00427.

Institutional Review Board Statement: Not applicable.

Data Availability Statement: No new data were created or analyzed in this study. Data sharing is not applicable to this article. The funders had no role in the design of the study; in the collection, analyses, or interpretation of data; in the writing of the manuscript; or in the decision to publish the results.

Acknowledgments: This research was performed at the Core Facility Centers “Development of Molecular and Cell Technologies” (electron microscopy), “Observatory of Environmental Safety” (culturing of marine invertebrates), and “Culture Collection of Microorganisms” (light microscopy) of the Research Park of Saint Petersburg University. Authors would like to thank the staff of the White Sea Biological Station of Moscow State University and the Educational and Research Station “Belomorskaia” of St Petersburg University for providing facilities for field sampling and material processing, as well as for their kind and friendly approach. GGP is especially grateful to Serge V. Bagrov and Maxim G. Vorobiev (St Petersburg University) for their technical assistance in field sampling and electron microscopy, respectively.

Conflicts of Interest: The authors declare no conflict of interest.

References

1. Janouškovec, J.; Paskerova, G.G.; Miroljubova, T.S.; Mikhailov, K.V.; Birley, T.; Aleoshin, V.V.; Simdyanov, T.G. Apicomplexan-like parasites are polyphyletic and widely but selectively dependent on cryptic plastid organelles. *eLife* **2019**, *8*, e49662. [[CrossRef](#)] [[PubMed](#)]
2. Simdyanov, T.G.; Paskerova, G.G.; Valigurová, A.; Diakin, A.; Kováčiková, M.; Schrével, J.; Guillou, L.; Dobrovolskij, A.A.; Aleoshin, V.V. First ultrastructural and molecular phylogenetic evidence from the blastogregarines, an early branching lineage of plesiomorphic Apicomplexa. *Protist* **2018**, *169*, 697–726. [[CrossRef](#)] [[PubMed](#)]
3. Kheisin, E.M. About the system of sporozoans (class Sporozoa, phylum Protozoa). *Zool. Zhurnal* **1956**, *35*, 1281–1298. (In Russian)
4. Perkins, F.O.; Barta, J.R.; Clopton, R.E.; Peirce, M.A.; Upton, S.J. Phylum Apicomplexa Levine, 1970. In *An Illustrated Guide to the Protozoa*, 2nd ed.; Lee, J.J., Leedale, G.F., Bradbury, P., Eds.; Society of Protozoologists: Lawrence, KS, USA, 2000; Volume 11, pp. 190–369.
5. Mathur, V.; Kwong, W.K.; Husnik, F.; Irwin, N.A.T.; Kristmundsson, A.; Gesta, C.; Freeman, M.; Keeling, P.J. Phylogenomics identifies a new major subgroup of apicomplexans, Marosporida *class nov.*, with extreme apicoplast genome reduction. *Genome Biol. Evol.* **2020**, *13*, evaa244. [[CrossRef](#)]
6. Mathur, V.; Wakeman, K.C.; Keeling, P.J. Parallel functional reduction in the mitochondria of apicomplexan parasites. *Curr. Biol.* **2021**, *31*, 2920–2928. [[CrossRef](#)]
7. Mathur, V.; Salomaki, E.D.; Wakeman, K.C.; Na, I.; Kwong, W.; Kolisko, M.; Keeling, P.J. Reconstruction of Plastid Proteomes of Apicomplexans and Close Relatives Reveals the Major Evolutionary Outcomes of Cryptic Plastids. *Mol. Biol. Evol.* **2023**, *40*, msad002. [[CrossRef](#)]
8. Brasil, L. *Eleutheroschizon duboscqi*, sporozoaire nouveau parasite de *Scoloplos armiger* O.F. Müller. *Arch. Zool. Exp. Gen.* **1906**, *4*, 17–22.
9. Chatton, E.; Villeneuve, F. Le cycle évolutif de l'*Eleutheroschizon duboscqui* Brasil. Prevue expérimentale de l'absence de schizogonie chez la *Siedleckia caulleryi* Ch et Vill. *C.R. Acad. Sci. D Nat.* **1936**, *203*, 834–837.
10. Valigurová, A.; Paskerova, G.G.; Diakin, A.; Kováčiková, M.; Simdyanov, T.G. Protococcidian *Eleutheroschizon duboscqi*, an unusual apicomplexan interconnecting gregarines and cryptosporidians. *PLoS ONE* **2015**, *10*, e0125063. [[CrossRef](#)]
11. Valigurová, A.; Jirku, M.; Koudela, B.; Gelnar, M.; Modry, D.; Slapeta, J. Cryptosporidia: Epicellular parasites embraced by the host cell membrane. *Int. J. Parasitol.* **2008**, *38*, 913–922. [[CrossRef](#)]
12. Kolářová, I.; Valigurová, A. Hide-and-peek: A game played between parasitic protists and their hosts. *Microorganisms* **2021**, *9*, 2434. [[CrossRef](#)]
13. Paskerova, G.G.; Miroljubova, T.S.; Diakin, A.; Kováčiková, M.; Valigurová, A.; Guillou, L.; Aleoshin, V.V.; Simdyanov, T.G. Fine structure and molecular phylogenetic position of two marine gregarines, *Selenidium pygospionis* sp. n. and *S. pherusa* sp. n., with notes on the phylogeny of Archigregarinida (Apicomplexa). *Protist* **2018**, *169*, 826–852. [[CrossRef](#)]
14. Edgar, R.C. MUSCLE: Multiple sequence alignment with high accuracy and high throughput. *Nucleic Acids Res.* **2004**, *32*, 1792–1797. [[CrossRef](#)]
15. Hall, T.A. BioEdit: A user-friendly biological sequence alignment editor and analysis program for Windows 95/98/NT. *Nucleic Acids Symp. Ser.* **1999**, *41*, 95–98.
16. Ronquist, F.; Teslenko, M.; van der Mark, P.; Ayres, D.L.; Darling, A.; Höhna, S.; Larget, B.; Liu, L.; Suchard, M.A.; Huelsenbeck, J.P. MrBayes 3.2: Efficient Bayesian phylogenetic inference and model choice across a large model space. *Syst. Biol.* **2012**, *61*, 539–542. [[CrossRef](#)]
17. Miller, M.A.; Pfeiffer, W.; Schwartz, T. Creating the CIPRES science gateway for inference of large phylogenetic trees. In *Gateway Computing Environments Workshop (GCE)*; IEEE: New Orleans, LA, USA, 2010; pp. 1–8. [[CrossRef](#)]
18. Minh, B.Q.; Schmidt, H.A.; Chernomor, O.; Schrempf, D.; Woodhams, M.D.; Von Haeseler, A.; Lanfear, R. IQ-TREE 2: New models and efficient methods for phylogenetic inference in the genomic era. *Mol. Biol. Evol.* **2020**, *37*, 1530–1534. [[CrossRef](#)]

19. Felsenstein, J. Phylogenies and the Comparative Method. *Am. Nat.* **1985**, *125*, 1–15. Available online: <http://www.jstor.org/stable/2461605> (accessed on 30 May 2023). [[CrossRef](#)]
20. Zuker, M. Mfold web server for nucleic acid folding and hybridization prediction. *Nucleic Acids Res.* **2003**, *31*, 3406–3415. [[CrossRef](#)]
21. Coleman, A.W. The significance of a coincidence between evolutionary landmarks found in mating affinity and a DNA sequence. *Protist* **2000**, *151*, 1–9. [[CrossRef](#)]
22. Coleman, A.W. Is there a molecular key to the level of “biological species” in eukaryotes? A DNA guide. *Mol. Phylogenet. Evol.* **2009**, *50*, 197–203. [[CrossRef](#)]
23. Müller, T.; Philippi, N.; Dandekar, T.; Schultz, J.; Wolf, M. Distinguishing species. *RNA* **2007**, *13*, 1469–1472. [[CrossRef](#)] [[PubMed](#)]
24. Wolf, M.; Chen, S.; Song, J.; Ankenbrand, M.; Müller, T. Compensatory base changes in ITS2 secondary structures correlate with the biological species concept despite intragenomic variability in ITS2 sequences—A proof of concept. *PLoS ONE* **2013**, *8*, e66726. [[CrossRef](#)] [[PubMed](#)]
25. Awerinzew, S. Studien über parasitische Protozoen. *Trav. Soc. Imper. Natur. St. Petersburg* **1908**, *38*, 1–139. (In Russian)
26. Word Register of Marine Species. Polychaeta. Available online: <https://www.marinespecies.org/aphia.php?p=taxdetails&id=883> (accessed on 30 May 2023).
27. Miroliubova, T.S.; Simdyanov, T.G.; Mikhailov, K.V.; Aleoshin, V.V.; Janouškovec, J.; Belova, P.A.; Paskerova, G.G. Polyphyletic origin, intracellular invasion, and meiotic genes in the putatively asexual agamococcidians (Apicomplexa incertae sedis). *Sci. Rep.* **2020**, *10*, 15847. [[CrossRef](#)] [[PubMed](#)]
28. Simdyanov, T.G.; Guillou, L.; Diakin, A.Y.; Mikhailov, K.V.; Schrével, J.; Aleoshin, V.V. A new view on the morphology and phylogeny of eugregarines suggested by the evidence from the gregarine *Ancora sagittata* (Leuckart, 1860) Labbé, 1899 (Apicomplexa: Eugregarinida). *PeerJ* **2017**, *5*, e3354. [[CrossRef](#)]
29. Schultz, J.; Maisel, S.; Gerlach, D.; Müller, T.; Wolf, M. A common core of secondary structure of the internal transcribed spacer 2 (ITS2) throughout the Eukaryota. *RNA* **2005**, *11*, 361–364. [[CrossRef](#)]
30. Huang, B.Q.; Chen, X.M.; LaRusso, N.F. *Cryptosporidium parvum* attachment to and internalization by human biliary epithelia in vitro: A morphologic study. *J. Parasitol.* **2004**, *90*, 212–221. [[CrossRef](#)]
31. Lumb, R.; Smith, K.; O’Donoghue, P.J.; Lanser, J.A. Ultrastructure of the attachment of *Cryptosporidium* sporozoites to tissue culture cells. *Parasitol. Res.* **1988**, *74*, 531–536. [[CrossRef](#)]
32. Valigurová, A.; Hofmannová, L.; Koudela, B.; Vávra, J. An ultrastructural comparison of the attachment sites between *Gregarina steini* and *Cryptosporidium muris*. *J. Eukaryot. Microbiol.* **2007**, *54*, 495–510. [[CrossRef](#)]
33. Umemiya, R.; Fukuda, M.; Fujisaki, K.; Matsui, T. Electron microscopic observation of the invasion process of *Cryptosporidium parvum* in severe combined immunodeficiency mice. *J. Parasitol.* **2005**, *91*, 1034–1039. [[CrossRef](#)]
34. Valigurová, A.; Florent, I. Nutrient acquisition and attachment strategies in basal lineages: A tough nut to crack in the evolutionary puzzle of Apicomplexa. *Microorganisms* **2021**, *9*, 1430. [[CrossRef](#)]
35. Bonnin, A.; Lapillonne, A.; Petrella, T.; Lopez, J.; Chaponnier, C.; Gabbiani, G.; Robine, S.; Dubremetz, J.F. Immunodetection of the microvillous cytoskeleton molecules villin and ezrin in the parasitophorous vacuole wall of *Cryptosporidium parvum* (Protozoa: Apicomplexa). *Eur. J. Cell Biol.* **1999**, *78*, 794–801. [[CrossRef](#)]
36. Melicherová, J.; Hofmannová, L.; Valigurová, A. Response of cell lines to actual and simulated inoculation with *Cryptosporidium proliferans*. *Eur. J. Protistol.* **2018**, *62*, 101–121. [[CrossRef](#)]
37. Barta, J.R.; Thompson, R.C.A. What is *Cryptosporidium*? Reappraising its biology and phylogenetic affinities. *Trends Parasitol.* **2006**, *22*, 463–468. [[CrossRef](#)]
38. Bartošová-Sojková, P.; Oppenheim, R.D.; Soldati-Favre, D.; Lukeš, J. Epicellular apicomplexans: Parasites “on the way in”. *PLoS Pathog.* **2015**, *11*, e1005080. [[CrossRef](#)]
39. Borowski, H.; Clode, P.L.; Thompson, R.C.A. Active invasion and/or encapsulation? A reappraisal of host-cell parasitism by *Cryptosporidium*. *Trends Parasitol.* **2008**, *24*, 509–516. [[CrossRef](#)]
40. Elliott, D.A.; Clark, D.P. *Cryptosporidium parvum* induces host cell actin accumulation at the host-parasite interface. *Infect. Immun.* **2000**, *68*, 2315–2322. [[CrossRef](#)]
41. Thompson, R.C.A.; Olson, M.E.; Zhu, G.; Enomoto, S.; Abrahamsen, M.S.; Hijjawi, N.S. *Cryptosporidium* and Cryptosporidiosis. *Adv. Parasitol.* **2005**, *59*, 77–158. [[CrossRef](#)]
42. Paskerova, G.G.; Miroliubova, T.S.; Valigurová, A.; Janouškovec, J.; Kováčiková, M.; Diakin, A.; Sokolova, Y.Y.; Mikhailov, K.V.; Aleoshin, V.V.; Simdyanov, T.G. Evidence from the resurrected family Polyrhadinidae Kamm, Apicomplexa: Gregarinomorpha supports the epimerite, an attachment organelle, as a major eugregarine innovation. *PeerJ* **2021**, *9*, e11912. [[CrossRef](#)]
43. Koreny, L.; Mercado-Saavedra, B.N.; Klinger, C.M.; Barylyuk, K.; Butterworth, S.; Hirst, J.; Rivera-Cuevas, Y.; Zaccari, N.R.; Holzer, V.J.C.; Klingl, A.; et al. Stable endocytic structures navigate the complex pellicle of apicomplexan parasites. *Nat. Commun.* **2023**, *14*, 2167. [[CrossRef](#)]
44. Piro, F.; Focaia, R.; Dou, Z.; Masci, S.; Smith, D.; Di Cristina, M. An uninvited seat at the dinner table: How apicomplexan parasites scavenge nutrients from the host. *Microorganisms* **2021**, *9*, 2592. [[CrossRef](#)] [[PubMed](#)]
45. Wan, W.; Dong, H.; Lai, D.H.; Yang, J.; He, K.; Tang, X.; Liu, Q.; Hide, G.; Zhu, X.Q.; Sibley, L.D.; et al. The *Toxoplasma* micropore mediates endocytosis for selective nutrient salvage from host cell compartments. *Nat. Commun.* **2023**, *14*, 977. [[CrossRef](#)] [[PubMed](#)]

46. Borowski, H.; Thompson, R.C.A.; Armstrong, T.; Clode, P.L. Morphological characterization of *Cryptosporidium parvum* life-cycle stages in an in vitro model system. *Parasitology* **2010**, *137*, 13–26. [[CrossRef](#)] [[PubMed](#)]
47. Frénal, K.; Dubremetz, J.F.; Lebrun, M.; Soldati-Favre, D. Gliding motility powers invasion and egress in Apicomplexa. *Nat. Rev. Microbiol.* **2017**, *15*, 645–660. [[CrossRef](#)]
48. Stoeck, T.; Kasper, J.; Bunge, J.; Leslin, C.; Ilyin, V.; Epstein, S. Protistan Diversity in the Arctic: A Case of Paleoclimate Shaping Modern Biodiversity? *PLoS ONE* **2007**, *2*, e728. [[CrossRef](#)]
49. Carreno, R.A.; Martin, D.S.; Barta, J.R. *Cryptosporidium* is more closely related to the gregarines than to coccidia as shown by phylogenetic analysis of apicomplexan parasites inferred using small-subunit ribosomal RNA gene sequences. *Parasitol. Res.* **1999**, *85*, 899–904. [[CrossRef](#)]
50. Mathur, V.; Kolisko, M.; Hehenberger, E.; Irwin, N.A.T.; Leander, B.S.; Kristmundsson, Á.; Freeman, M.A.; Keeling, P.J. Multiple independent origins of apicomplexan-like parasites. *Curr. Biol.* **2019**, *29*, 2936–2941. [[CrossRef](#)]
51. Salomaki, E.D.; Terpis, K.X.; Rueckert, S.; Kotyk, M.; Varadínová, Z.K.; Čepička, I.; Lane, C.E.; Kolisko, M. Gregarine single-cell transcriptomics reveals differential mitochondrial remodeling and adaptation in apicomplexans. *BMC Biol.* **2021**, *19*, 77. [[CrossRef](#)]

Disclaimer/Publisher’s Note: The statements, opinions and data contained in all publications are solely those of the individual author(s) and contributor(s) and not of MDPI and/or the editor(s). MDPI and/or the editor(s) disclaim responsibility for any injury to people or property resulting from any ideas, methods, instructions or products referred to in the content.